# Scanning the Earth with solar neutrinos and DUNE

Ara N. Ioannisian
YerPhI and ITPM, Armenia
Fermilab, Neutrino seminar

13 July, 2017

# Geophysics, Scan the Earth via solar boron neutrinos at DUNE

Ara Ioannisian, Alexei Smirnov and Daniel Wyler

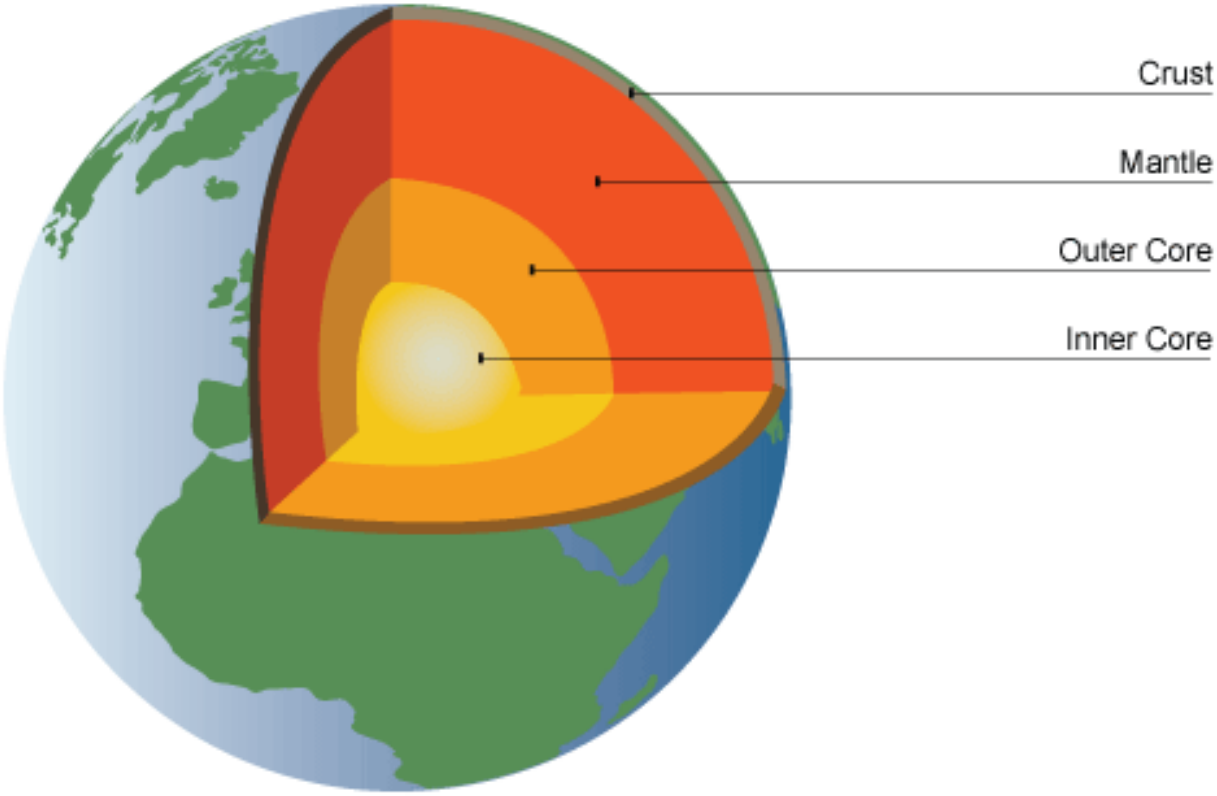
Crust
Mantle
Outer Core
Inner Core

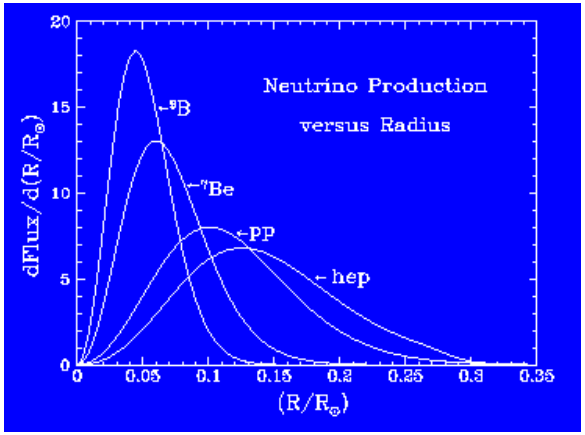


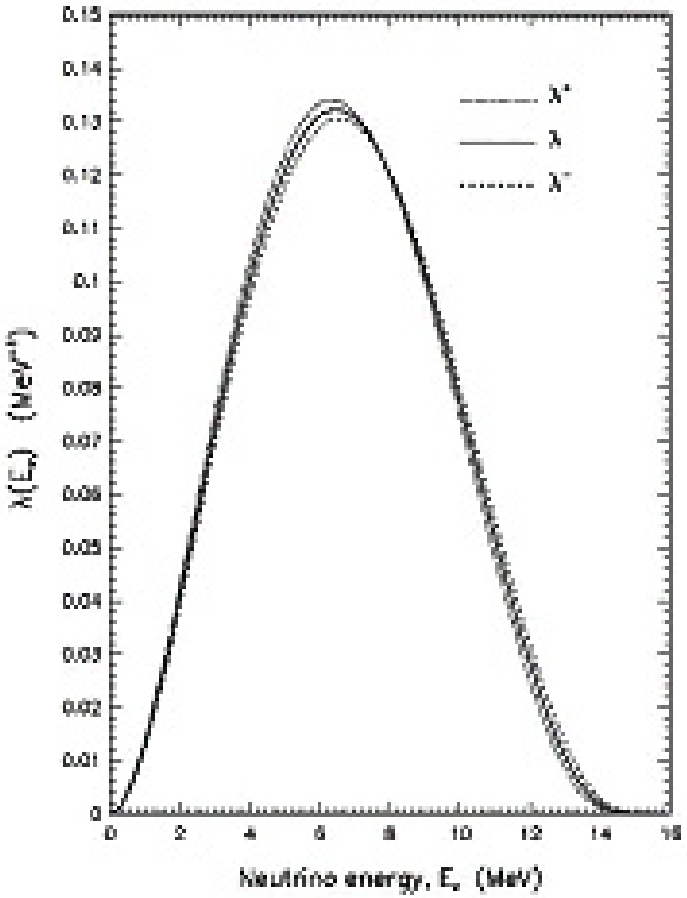


From the Earth $^8B$ neutrino production region in the Sun is seen as a very small disk with angular size $\approx 10^{-4}$

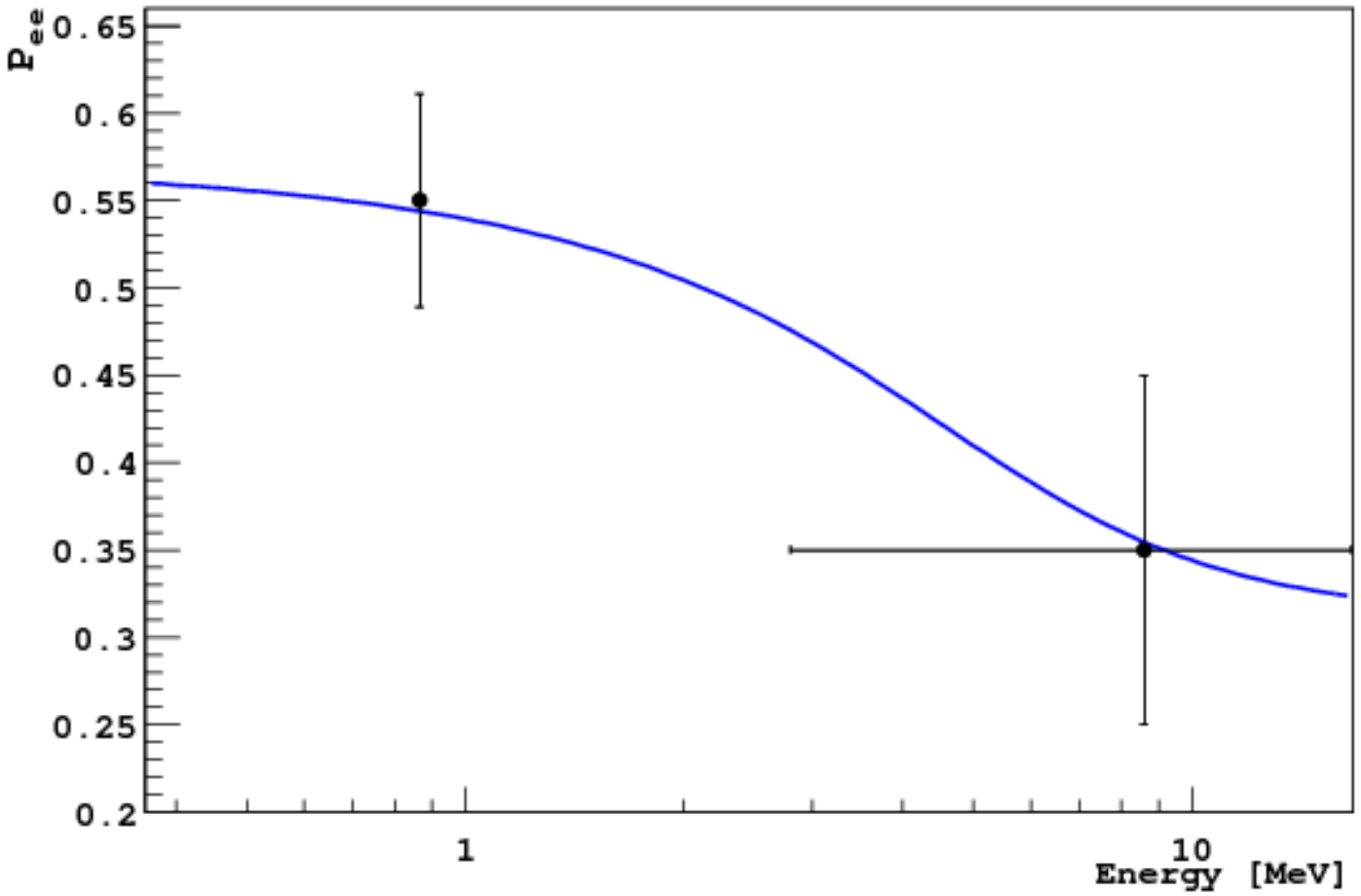


$$P_D \equiv P_{ee} = \frac{c_{13}^4}{2}(1 + \cos 2\bar{\theta}_{12}^{\odot} \cos 2\theta_{12}) + s_{13}^4 \simeq$$
$$c_{13}^2 s_{12}^2 + s_{14}^4 + \frac{1}{4} \cos 2\theta_{12} \sin^2 2\theta_{12} \left(\frac{\Delta m_{12}^2}{2EV_e^0}\right)^2 \simeq 0.32$$

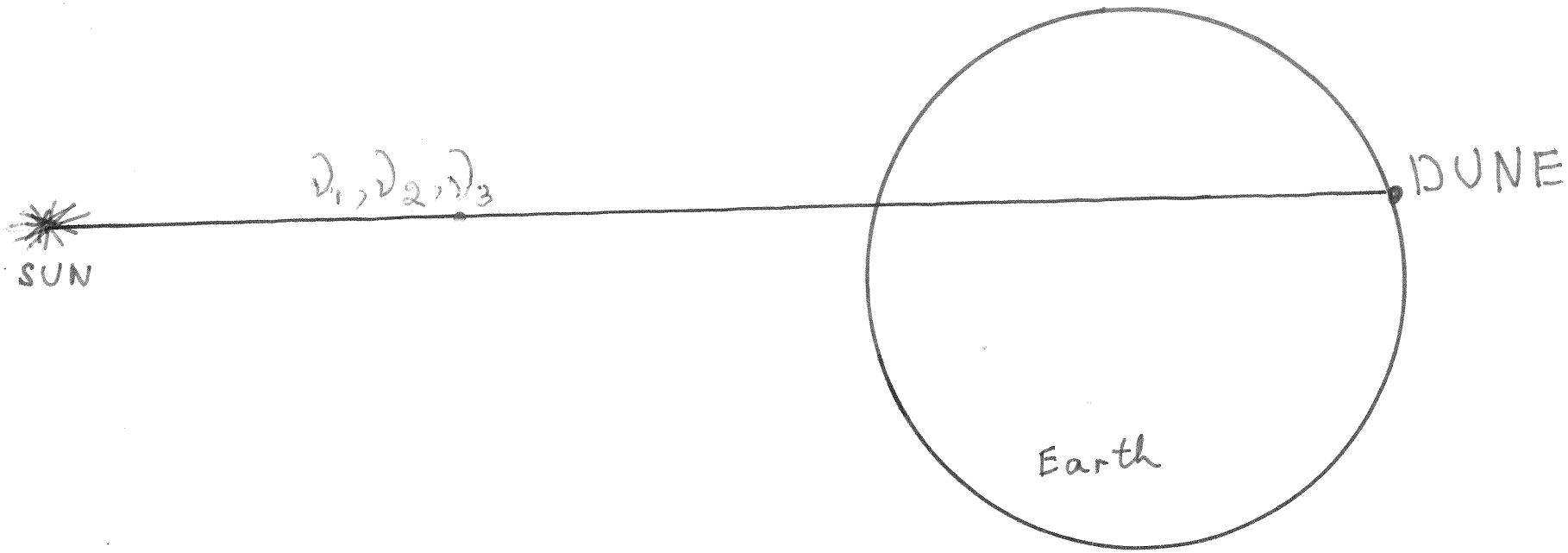
$\nu_1, \nu_2, \nu_3$
SUN
DUNE
Earth

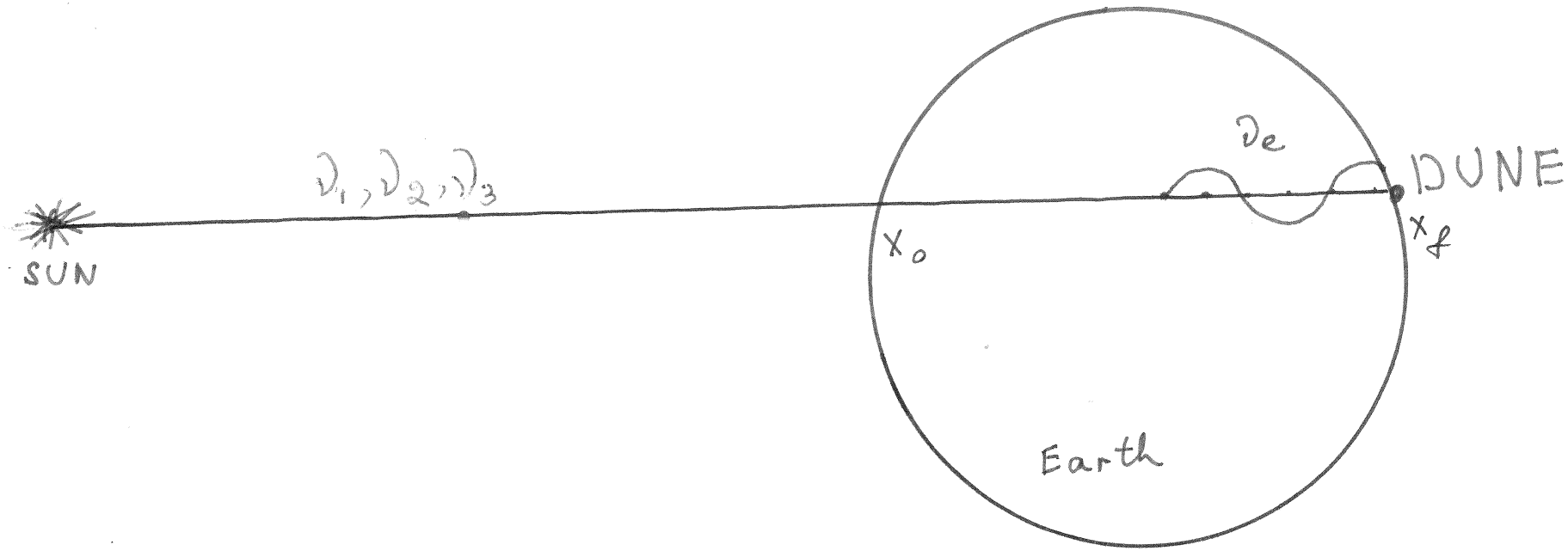


$$\Delta P_{\nu_2 \to \nu_e} = C\ \sqrt{2} G_F \int_{x_0}^{x_f} dx\ N_e(x)\ \sin \frac{\Delta m_{21}^2}{2E}(x_f - x)$$

$$\Delta P_{ee} = -\frac{c_{13}^2}{2}(2P_{ee} - c_{13}^4 - 2s_{13}^4)\frac{\sin^2 2\theta_{12}}{\cos 2\theta_{12}}\ \sqrt{2} G_F \int_{x_0}^{x_f} dx\ N_e(x) \sin \frac{\Delta m_{21}^2}{2E}(x_f - x)$$

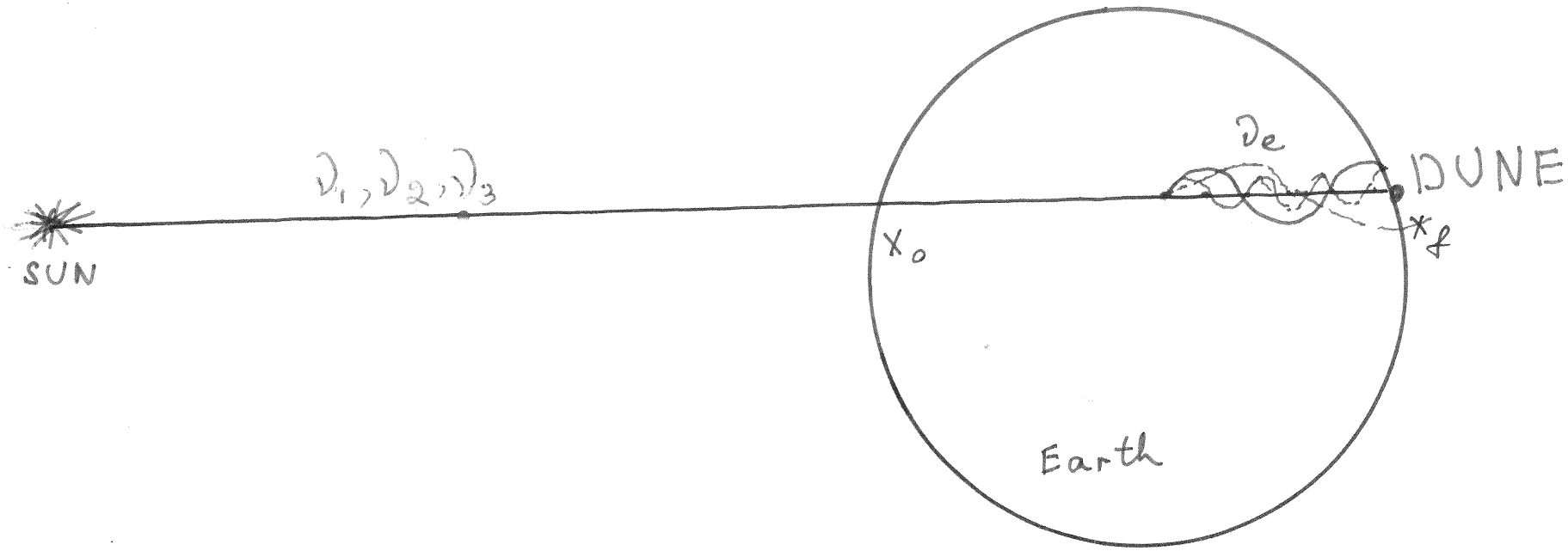


$$g(E, E') = \frac{1}{\sigma\sqrt{2\pi}} e^{-\frac{(E-E')^2}{2\sigma^2}}$$

$$\overline{\Delta P_{ee}} = -\frac{c_{13}^2}{2}(2P_{ee} - c_{13}^4 - 2s_{13}^4)\frac{\sin^2 2\theta_{12}}{\cos 2\theta_{12}} \sqrt{2} G_F \int_{x_0}^{x_f} dx\, F(x_f - x)\, N_e(x) \sin \frac{\Delta m_{21}^2}{2E}(x_f - x)$$

$$F(x_f - x) \simeq e^{-2(\frac{\pi\sigma(x_f - x)}{E\ l_\nu})^2}$$

There are several matter density jumps in the Earth.
Within those jumps matter density changes weakly $\rightarrow$ adiabatic conditions of neutrino oscillation is held within layers between density jumps.

$$\begin{aligned}\Delta P_{ee} &= -\frac{2P_{ee} - c_{13}^4 - 2s_{13}^4}{\cos 2\theta_{12}} \\ &\{-\sin^2\theta_{12} - \sin 2\theta_{12}^s \sin(-2\theta_{12}^s + 2\theta_{12}) \sin^2\frac{\Phi}{2} \\ &-2\sin(-4\theta_{12}^s + 2\theta_{12}) \sin\frac{\Phi}{2} \sum \Delta\theta_{12}^i \sin\phi_i \ \}\end{aligned}$$

$\theta_{12}^s$ mixing angle at surface,
$\Phi$ full phase in the Earth,
$\Delta\theta_{12}^i$ jump of the mixing angle at the interface of different layers of the Earth,
$\phi_i$ phase from the density jump to the detector

SK Day-Night effect  Phys.Rev.Lett. 112, 091805 (2014)

| | $A_{\mathrm{DN}} \pm (\mathrm{stat}) \pm (\mathrm{syst})$ | $A_{\mathrm{DN}}^{\mathrm{fit}} \pm (\mathrm{stat}) \pm (\mathrm{syst})$ |
|---|---|---|
| SK-I | $(-2.1 \pm 2.0 \pm 1.3)\%$ | $(-2.0 \pm 1.7 \pm 1.0)\%$ |
| SK-II | $(-5.5 \pm 4.2 \pm 3.7)\%$ | $(-4.3 \pm 3.8 \pm 1.0)\%$ |
| SK-III | $(-5.9 \pm 3.2 \pm 1.3)\%$ | $(-4.3 \pm 2.7 \pm 0.7)\%$ |
| SK-IV | $(-5.3 \pm 2.0 \pm 1.4)\%$ | $(-3.4 \pm 1.8 \pm 0.6)\%$ |
| Combined | $(-4.2 \pm 1.2 \pm 0.8)\%$ | $(-3.2 \pm 1.1 \pm 0.5)\%$ |

for fit they use $\Delta m^2 = 4.8^{+1.8}_{-0.9}\ 10^{-5} eV^2$, $\theta_{12} = 35.8^0 \pm$, $\theta_{13} = 9.1^0$
KamLAND $\Delta m^2 = 7.5\ 10^{-5} eV^2$ one expects at SK $A_{DN} = -2.1\%$
Thus SK sees 2 (fitted 1.5) times larger effect $\rightarrow$ 2 (1.5) times larger electron density
mater density is known $\rightarrow$ chemical composition
Therefore there is more (much more) hydrogen must be in the Earth in order to explain SK DN result

Liquid Argon detectors.

$$A_e(E) = \frac{\int dE' g(E,E')\ \sigma_{\nu Ar}(E') f_{B8}(E') \Delta P_{ee}(E')}{\int dE' g(E,E')\ \sigma_{\nu Ar}(E') f_{B8}(E') P_{ee}(E')}$$

$$\Delta P_{ee} = -\frac{c_{13}^2}{2}(2P_D - c_{13}^4 - 2s_{13}^4)\frac{\sin^2 2\theta_{12}}{\cos 2\theta_{12}}\sqrt{2}G_F\int_0^L dx\ N_e(x)\sin\frac{\Delta m_{21}^2}{2E}(L-x)$$

$$f_{B^8}(E_\nu) = C\ E_\nu^2\ (E_\nu^{max} - E_\nu + m_e)\ \sqrt{(E_\nu^{max} - E_\nu + m_e)^2 - m_e^2}$$

$E_\nu^{max} \simeq 14.1$ MeV.

$$C = 260\ \frac{\mathrm{Flux}_{B^8}}{5.7\ 10^6\ cm^{-2}sec^{-1}}\frac{1}{\mathrm{MeV}^5}\frac{1}{cm^2 sec}$$

About 9.7% of $B^8$ neutrinos have energy $E_\nu > 11$ MeV and 0.96 % have energy above $E_\nu > 13$ MeV.

$$g(E,E') = \frac{1}{\sigma_E\sqrt{2\pi}}e^{-\frac{(E-E')^2}{2\sigma_E^2}}$$

$^{40}$Ar has 0 spin and $^{40}$K has 4 spin. Therefore it is highly suppressed direct transition via weak current $W$ exchange. That transition becomes allowed via intermediate states, excitation states of $^{40}$K, and farther emission of photons. These transition probabilities are not measured yet. In our numerical study we'll approximate to

$$\sigma_{\nu_e Ar} \simeq 2\ 10^{-43}\mathrm{cm}^2 \frac{p_e E_e}{\mathrm{MeV}}$$

where $E_e = E_\nu - 5.8\mathrm{MeV}$.

In our computations we used the spherically symmetric Earth PREM model ( density jumps at 15, 25, 210, 400, 670, 2830 and 5150 km from the surface of the Earth.
Trajectories with $\eta < 0.58$ cross the core of the Earth.
Annually we expect about 27000 registered electron neutrinos ($E_\nu$ >11 MeV ) at 40kt liquid argon detector due to the reaction

$$\nu_e +^{40} Ar \rightarrow^{40} K + e^-$$

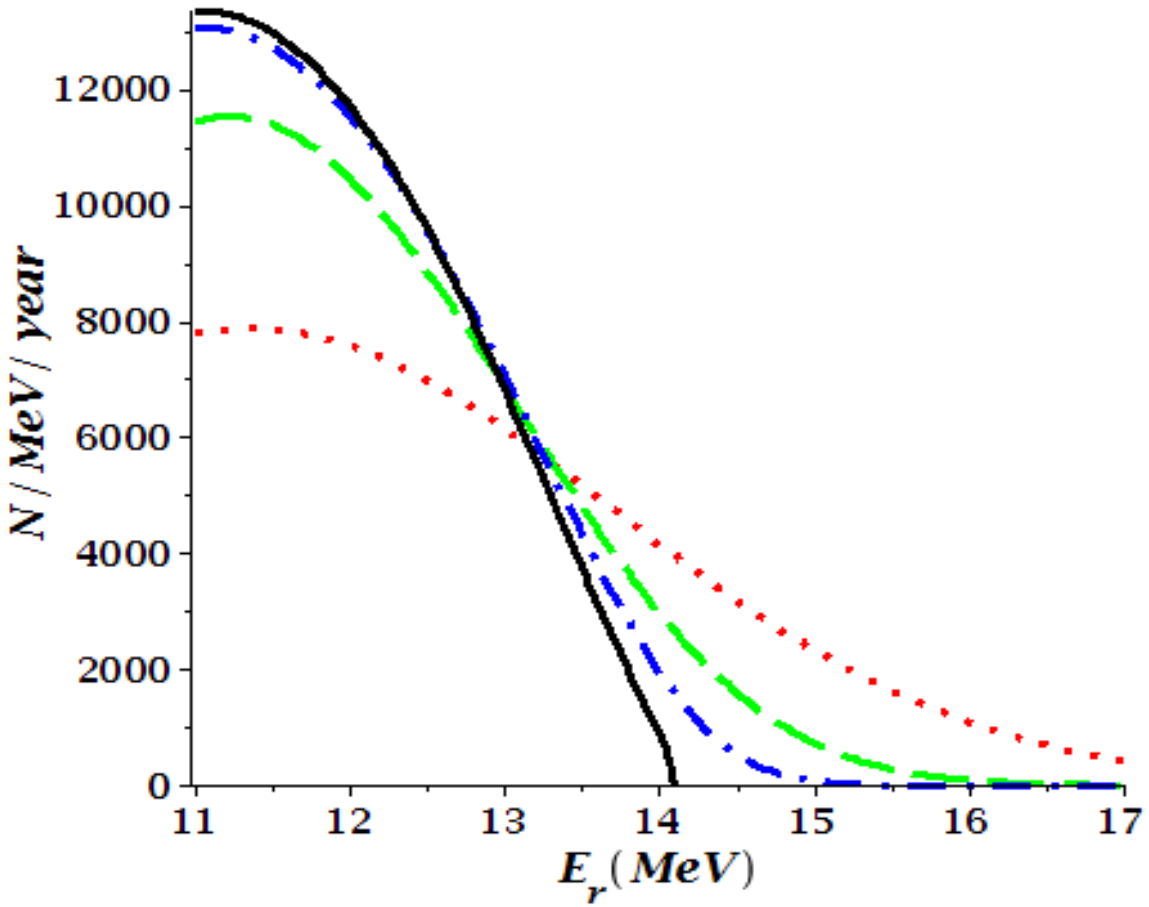


Figure: (Annually expected) registered neutrino spectrum on reconstructed neutrino energy ($E_r$). The number of expected total registered neutrinos with energy $E_r > 11$ MeV is about 27000 and it almost does not depend on energy resolution of the detector. solid line (black) -exact neutrino spectrum, dot line (blue) - 0.5 MeV resolution, dash line (green) - 1 MeV resolution, dash-dot line (red) -2 MeV resolution.

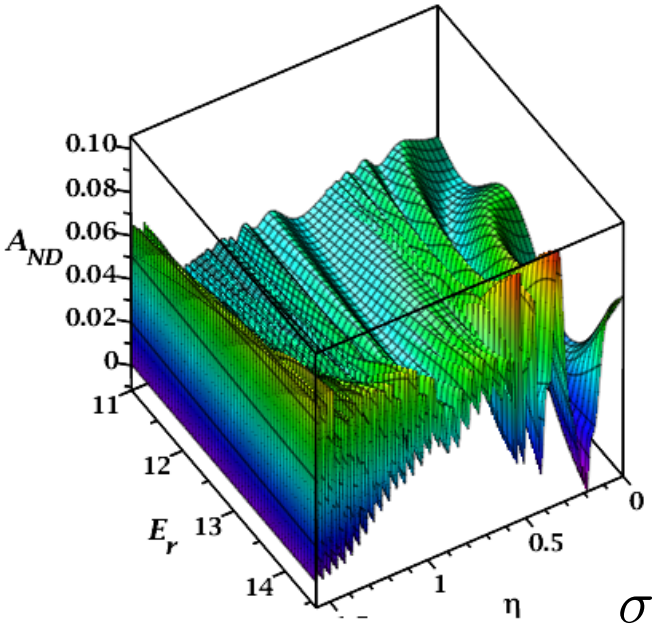


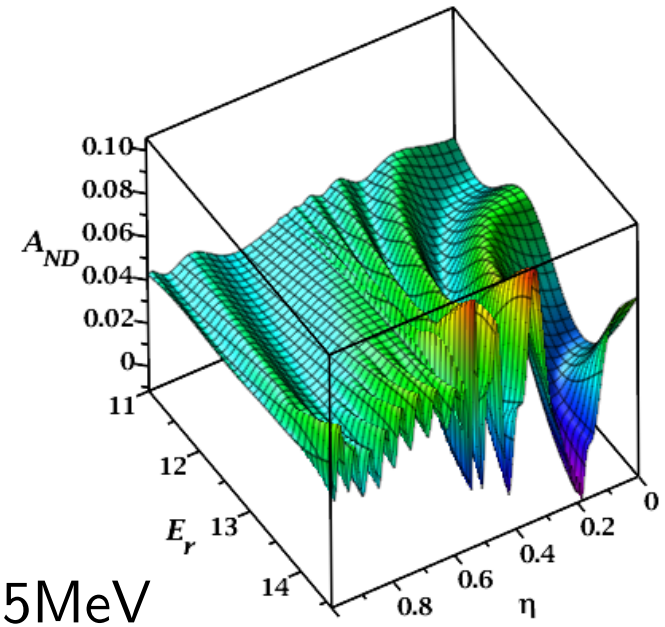


- $\sigma_E$=0.5MeV

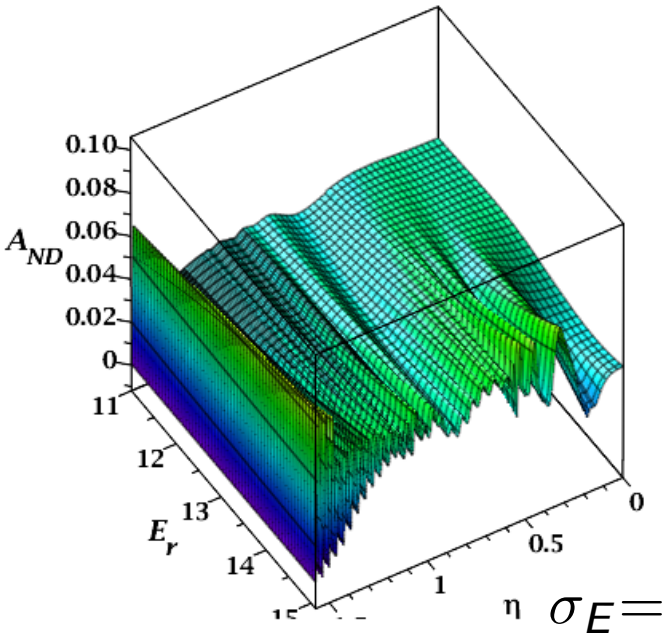


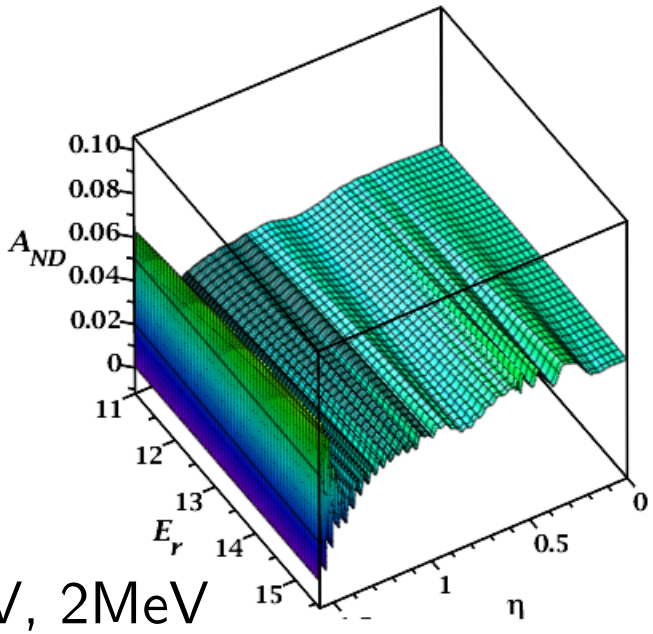


$\sigma_E$=1MeV, 2MeV

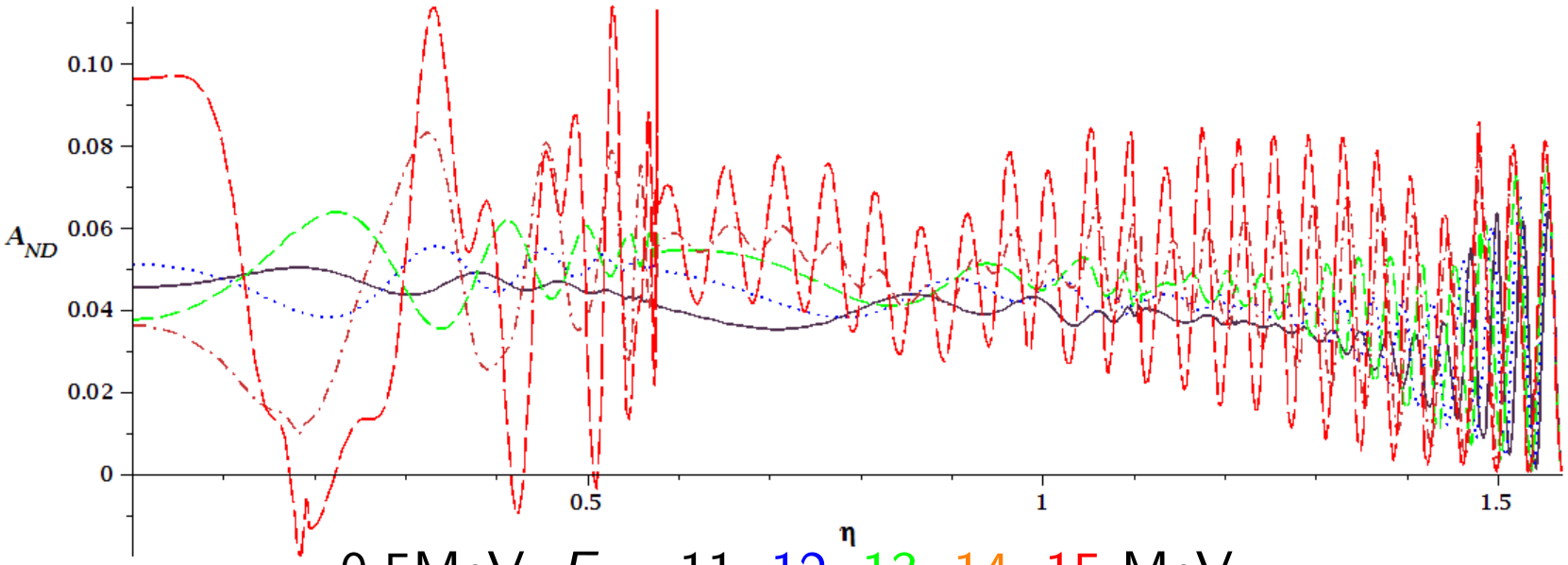


$\sigma_E$=0.5MeV, $E_r$= 11 ,12 ,13 ,14 ,15 MeV

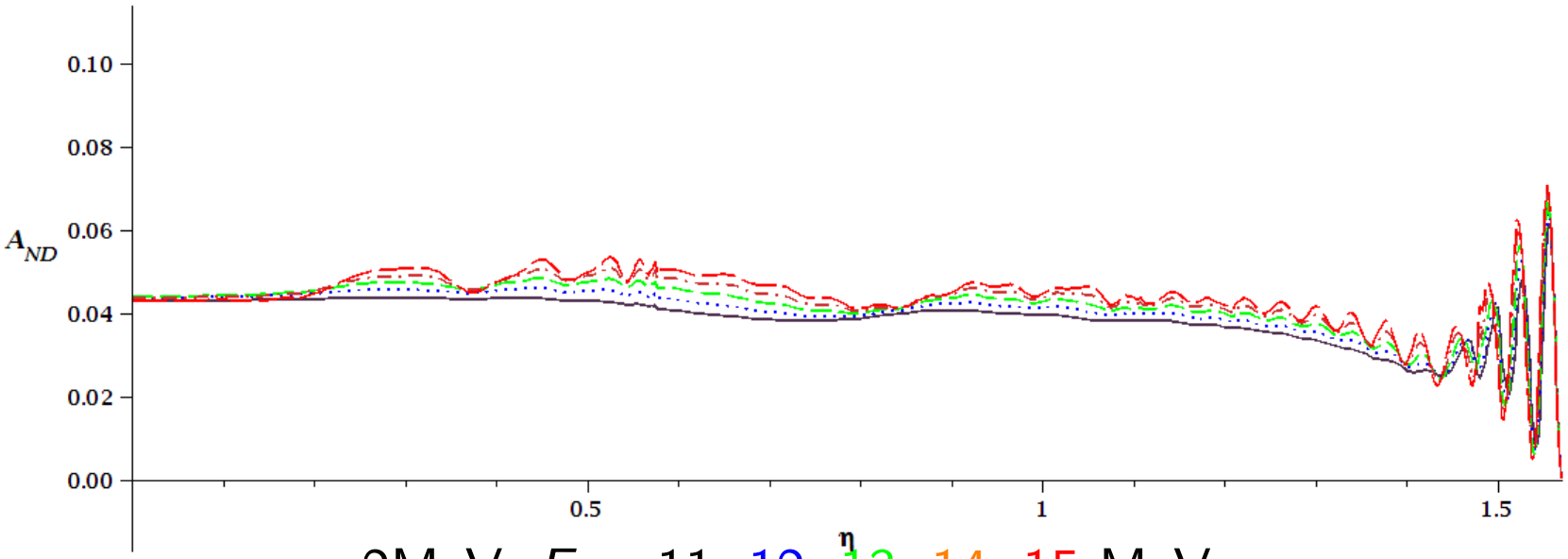


$\sigma_E$=2MeV, $E_r$= 11 ,12 ,13 ,14 ,15 MeV

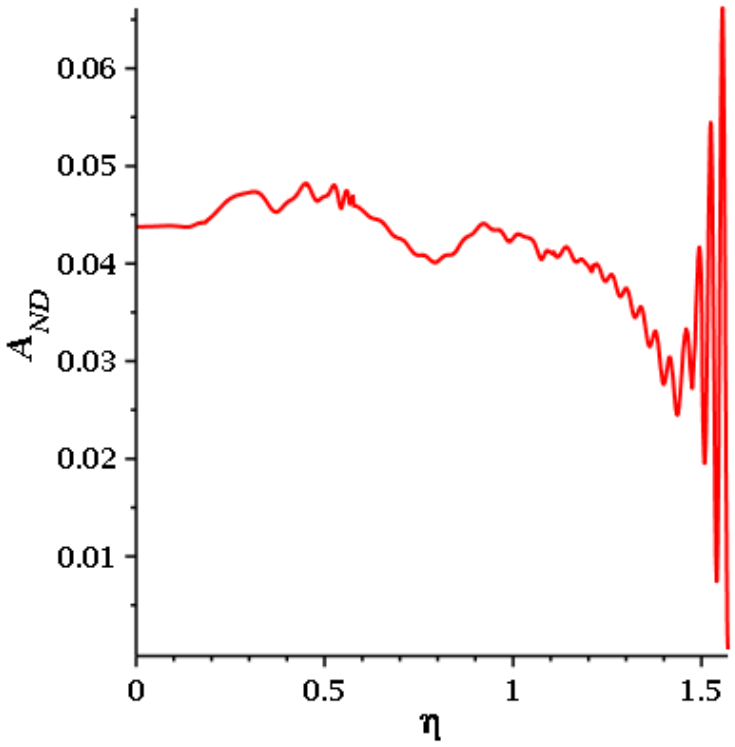


Figure: The relative variation of the boron solar neutrino flux with energy $E_r$ >11 MeV as function of the nadir angle of the neutrino trajectory.

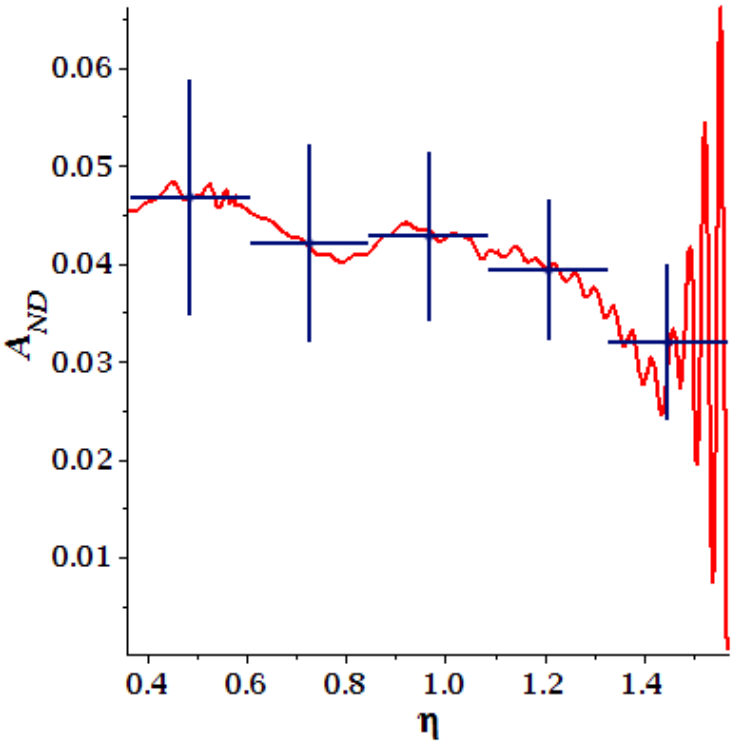
0.06
0.05
0.04
0.03
0.02
0.01
$A_{ND}$
0.4
0.6
0.8
1.0
1.2
1.4
η

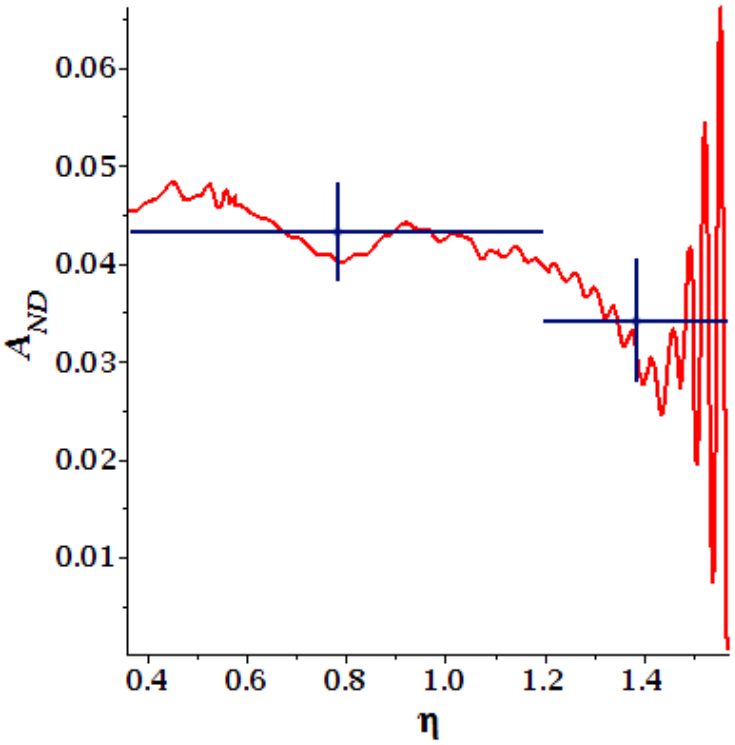
0.06
0.05
0.04
0.03
0.02
0.01
$A_{ND}$
0.4
0.6
0.8
1.0
1.2
1.4
η

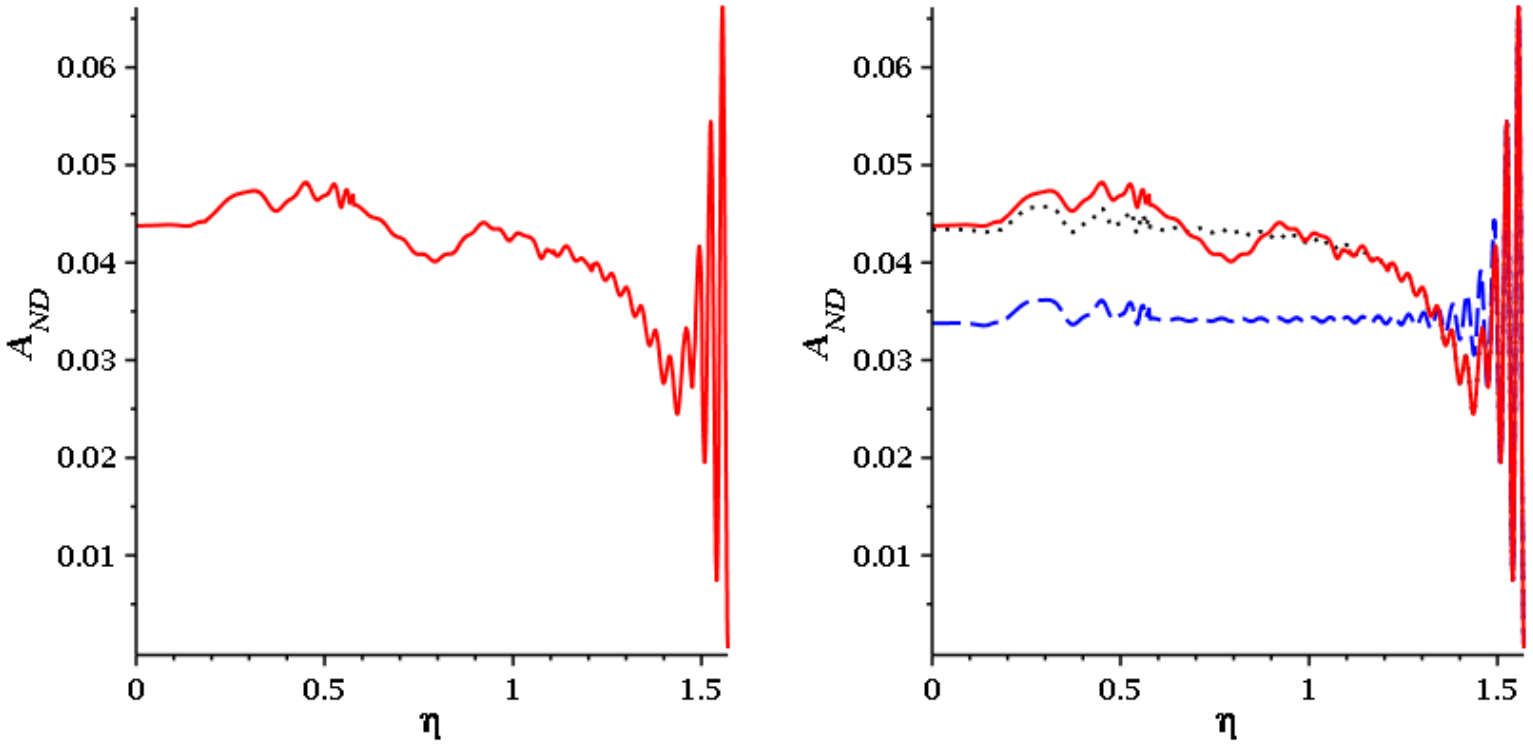
0.06
0.05
0.04
0.03
0.02
0.01
$A_{ND}$
0
0.5
1
1.5
η
0.06
0.05
0.04
0.03
0.02
0.01
$A_{ND}$
0
0.5
1
1.5
η

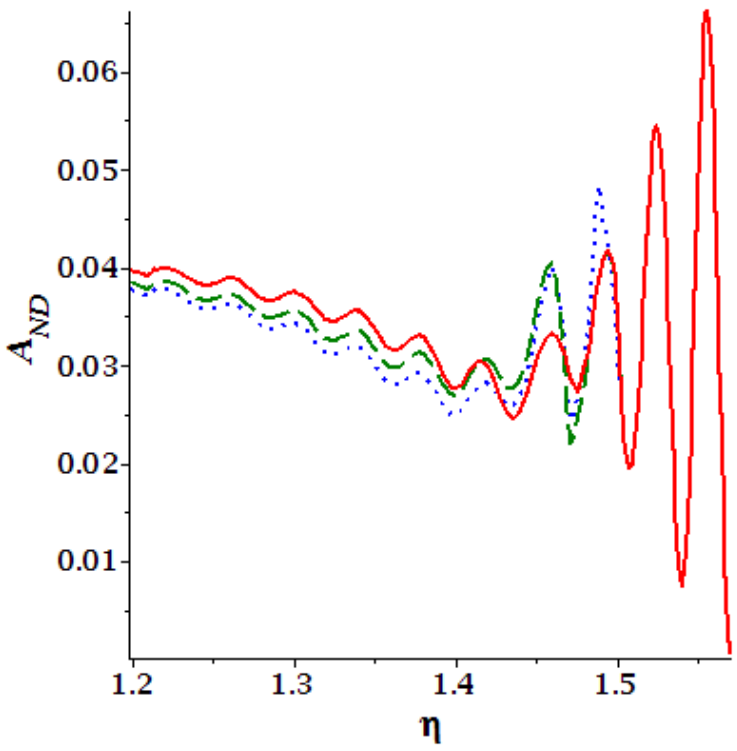


Figure: The relative excess of night events integrated over $E_r$ >11 MeV as function of the nadir angle of the neutrino trajectory for changed parameters of density jumps. Red line is the old one with jumps at 15 km and 25 km; blue-dotted line is for jumps at $h_1 = 20.5$ km and $h_2 = 30$ km; green-dashed line is for jumps at $h_1 = 15$ , $h_2 = 30$. Parametric enhancement of oscillations is seen in the 3rd and 4th periods.

CONCLUSIONS

- Water Cherenkov or scintillator detectors are "shortsighted".
- DUNE is an unique instrument to scan the Earth
- At night time the regeneration of $\nu_e$ (11MeV $< E_\nu <$14 MeV ) is 4 %, with modulation up to 10 %. One year of taking data from one 10 kt module of DUNE far detector will determine the Earth matter effect at 2.6 $\sigma$ c.l. (SuperKamiokande reached that result after 20 years of taking data). After 10 years of taking data from all 4 DUNE modules the Earth matter effect will be determined in more than 16 $\sigma$ c.l.
- Good energy resolution ($\sigma < 7\% E_\nu$) will make it possible to measure electron densite at deep layers of the Earth and with the known density profile of the Earth learn about the chemical composition of the Earth's interior.

THANK YOU

| Preliminary Reference Earth Model (PREM) (Dziewonski & Anderson, 1981) | | | | | | | | | |
|---|---|---|---|---|---|---|---|---|---|
| Region | Radius (km) | $\alpha$ (m/s) | $\beta$ (m/s) | $\rho$ (kg/m3) | $K_s$ (Gpa) | $\mu$ (Gpa) | $\nu$ | P (Gpa) | g (m/s2) |
| Inner Core | 0 | 11266.2 | 3667.8 | 13088.48 | 1425.3 | 176.1 | 0.4407 | 363.85 | 0 |
| | 200 | 11255.93 | 3663.42 | 13079.77 | 1423.1 | 175.5 | 0.4408 | 362.9 | 0.7311 |
| | 400 | 11237.12 | 3650.27 | 13053.64 | 1416.4 | 173.9 | 0.441 | 360.03 | 1.4604 |
| | 600 | 11205.76 | 3628.35 | 13010.09 | 1405.3 | 171.3 | 0.4414 | 355.28 | 2.1862 |
| | 800 | 11161.86 | 3597.67 | 12949.12 | 1389.8 | 167.6 | 0.442 | 348.67 | 2.9068 |
| | 1000 | 11105.42 | 3558.23 | 12870.73 | 1370.1 | 163 | 0.4428 | 340.24 | 3.6203 |
| | 1200 | 11036.43 | 3510.02 | 12774.93 | 1346.2 | 157.4 | 0.4437 | 330.05 | 4.3251 |
| | 1221.5 | 11028.27 | 3504.32 | 12763.6 | 1343.4 | 156.7 | 0.4438 | 328.85 | 4.4002 |
| Outer Core | 1221.5 | 10355.68 | 0 | 12166.34 | 1304.7 | 0 | 0.5 | 328.85 | 4.4002 |
| | 1400 | 10249.59 | 0 | 12069.24 | 1267.9 | 0 | 0.5 | 318.75 | 4.9413 |
| | 1600 | 10122.91 | 0 | 11946.82 | 1224.2 | 0 | 0.5 | 306.15 | 5.5548 |
| | 1800 | 9985.54 | 0 | 11809 | 1177.5 | 0 | 0.5 | 292.22 | 6.1669 |
| | 2000 | 9834.96 | 0 | 11654.78 | 1127.3 | 0 | 0.5 | 277.04 | 6.7715 |
| | 2200 | 9668.65 | 0 | 11483.11 | 1073.5 | 0 | 0.5 | 260.68 | 7.3645 |
| | 2400 | 9484.09 | 0 | 11292.98 | 1015.8 | 0 | 0.5 | 243.25 | 7.9425 |
| | 2600 | 9278.76 | 0 | 11083.35 | 954.2 | 0 | 0.5 | 224.85 | 8.5023 |
| | 2800 | 9050.15 | 0 | 10853.21 | 888.9 | 0 | 0.5 | 205.6 | 9.0414 |
| | 3000 | 8795.73 | 0 | 10601.52 | 820.2 | 0 | 0.5 | 185.64 | 9.557 |
| | 3200 | 8512.98 | 0 | 10327.26 | 748.4 | 0 | 0.5 | 165.12 | 10.0464 |
| | 3400 | 8199.39 | 0 | 10029.4 | 674.3 | 0 | 0.5 | 144.19 | 10.5065 |
| | 3480 | 8064.82 | 0 | 9903.49 | 644.1 | 0 | 0.5 | 135.75 | 10.6823 |
| D'' | 3480 | 13716.6 | 7264.66 | 5566.45 | 655.6 | 293.8 | 0.3051 | 135.75 | 10.6823 |
| | 3600 | 13687.53 | 7265.75 | 5506.42 | 644 | 290.7 | 0.3038 | 128.71 | 10.5204 |
| | 3630 | 13680.41 | 7265.97 | 5491.45 | 641.2 | 289.9 | 0.3035 | 126.97 | 10.4844 |
| Lower mantle | 3630 | 13680.41 | 7265.97 | 5491.45 | 641.2 | 289.9 | 0.3035 | 126.97 | 10.4844 |
| | 3800 | 13447.42 | 7188.92 | 5406.81 | 609.5 | 279.4 | 0.3012 | 117.35 | 10.3095 |
| | 4000 | 13245.32 | 7099.74 | 5307.24 | 574.4 | 267.5 | 0.2984 | 106.39 | 10.158 |
| | 4200 | 13015.79 | 7010.53 | 5207.13 | 540.9 | 255.9 | 0.2957 | 95.76 | 10.0535 |
| | 4400 | 12783.89 | 6919.57 | 5105.9 | 508.5 | 244.5 | 0.2928 | 85.43 | 9.9859 |
| | 4600 | 12544.66 | 6825.12 | 5002.99 | 476.6 | 233.1 | 0.2898 | 75.36 | 9.9474 |
| | 4800 | 12293.16 | 6725.48 | 4897.83 | 444.8 | 221.5 | 0.2864 | 65.52 | 9.9314 |
| | 5000 | 12024.45 | 6618.91 | 4789.83 | 412.8 | 209.8 | 0.2826 | 55.9 | 9.9326 |
| | 5200 | 11733.57 | 6563.7 | 4678.44 | 380.3 | 197.9 | 0.2783 | 46.49 | 9.9467 |
| | 5400 | 11415.6 | 6378.13 | 4563.07 | 347.1 | 185.6 | 0.2731 | 37.29 | 9.9698 |
| | 5600 | 11065.57 | 6240.46 | 4443.17 | 313.3 | 173 | 0.2668 | 28.29 | 9.9985 |
| | 5600 | 11065.57 | 6240.46 | 4443.17 | 313.3 | 173 | 0.2668 | 28.29 | 9.9985 |
| | 5701 | 10751.31 | 5945.08 | 4380.71 | 299.9 | 154.8 | 0.2798 | 23.83 | 10.0143 |
| Transition Zone | 5701 | 10266.22 | 5570.2 | 3992.14 | 255.6 | 123.9 | 0.2914 | 23.83 | 10.0143 |
| | 5771 | 10157.82 | 5516.01 | 3975.84 | 248.9 | 121 | 0.2909 | 21.04 | 10.0038 |
| | 5871 | 9645.88 | 5224.28 | 3849.8 | 218.1 | 105.1 | 0.2924 | 17.13 | 9.9883 |
| | 5971 | 9133.97 | 4932.59 | 3723.78 | 189.9 | 90.6 | 0.2942 | 13.35 | 9.9686 |
| | 5971 | 8905.22 | 4769.89 | 3543.25 | 173.5 | 80.6 | 0.2988 | 13.35 | 9.9686 |
| | 6061 | 8732.09 | 4706.9 | 3489.51 | 163 | 77.3 | 0.2952 | 10.2 | 9.9361 |
| | 6151 | 8558.96 | 4643.91 | 3435.78 | 152.9 | 74.1 | 0.2914 | 7.11 | 9.9048 |
| Low Velocity Zone | 6151 | 7989.7 | 4418.85 | 3359.5 | 127 | 65.6 | 0.2797 | 7.11 | 9.9048 |
| | 6221 | 8033.7 | 4443.61 | 3367.1 | 128.7 | 66.5 | 0.2796 | 4.78 | 9.8783 |
| | 6291 | 8076.88 | 4469.53 | 3374.71 | 130.3 | 67.4 | 0.2793 | 2.45 | 9.8553 |
| Lid | 6291 | 8076.88 | 4469.53 | 3374.71 | 130.3 | 67.4 | 0.2793 | 2.45 | 9.8553 |
| | 6346.6 | 8110.61 | 4490.94 | 3380.76 | 131.5 | 68.2 | 0.2789 | 0.604 | 9.8394 |
| Crust | 6346.6 | 6800 | 3900 | 2900 | 75.3 | 44.1 | 0.2549 | 0.604 | 9.8394 |
| | 6356 | 6800 | 3900 | 2900 | 75.3 | 44.1 | 0.2549 | 0.337 | 9.8332 |
| | 6356 | 5800 | 3200 | 2600 | 52 | 26.6 | 0.2812 | 0.337 | 9.8332 |
| | 6368 | 5800 | 3200 | 2600 | 52 | 26.6 | 0.2812 | 0.3 | 9.8222 |
| Ocean | 6368 | 1450 | 0 | 1020 | 2.1 | 0 | 0.5 | 0.3 | 9.8222 |
| | 6371 | 1450 | 0 | 1020 | 2.1 | 0 | 0.5 | 0 | 9.8156 |

Averaging over neutrino energy

$$A_e = \int dE' g(E', E) \frac{P_N - P_D}{P_D} \ .$$

$$A_e = -f(\Delta m^2_{21}, \theta_{12}) \frac{1}{2} \int_0^L dx \ V(x) F(L-x) \sin \phi^m_{x \to L},$$

The decrease of $F$ means that contributions from the large distances to the integral are suppressed.

Gaussian energy resolution function

$$g(E, E') = \frac{1}{\sigma\sqrt{2\pi}} e^{-\frac{(E-E')^2}{2\sigma^2}}, \qquad F(L-x) \simeq e^{-2(\frac{\pi\sigma(L-x)}{E \ l_\nu})^2}$$

Box like energy resolution function

$$A_e = \frac{1}{2\sigma} \int_{E-\sigma}^{E+\sigma} dE' \ \frac{P_N - P_D}{P_D}$$

$$F(L-x) \simeq \frac{1}{Q(L-x)} \sin Q(L-x), \qquad Q(L-x) \equiv \frac{2\pi\sigma(L-x)}{E \ l_\nu} \ ,$$

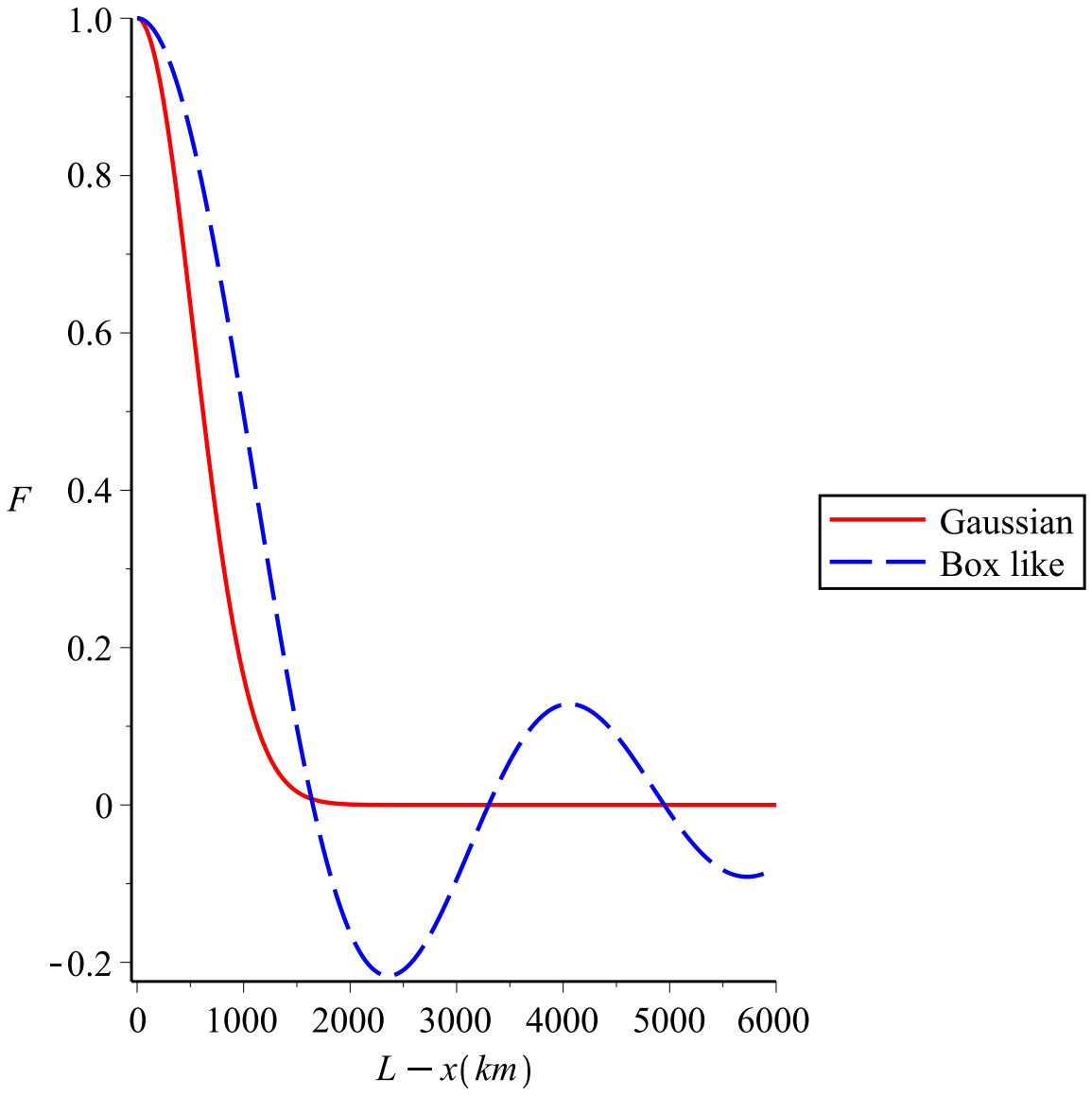


The attenuation factor $F$ as function of $(L - x)$ (distance from detector). $E = 10$ MeV, $\sigma = 1$ MeV, and $\Delta m^2_{21} = 7.5 \cdot 10^{-5}$ eV$^2$.

## WC

$$A_e(T,\eta) = \frac{\int dT'\ g(T,T') \int_{T+\frac{m_e}{2}} dE\ \Delta P_{ee}(E) j_B(E) (\frac{d\sigma_{\nu_e e}}{dT'} - \frac{d\sigma_{\nu_\alpha e}}{dT'})}{\int dT'\ g(T,T') \int_{T+\frac{m_e}{2}} dE\ j_B(E) (P_{ee} \frac{d\sigma_{\nu_e e}}{dT'} + (1-P_{ee}) \frac{d\sigma_{\nu_\alpha e}}{dT'})}$$

$$\Delta P_{ee} = P_N - P_D = -\frac{c_{13}^2}{2}(2P_{ee} - c_{13}^4 - 2s_{13}^4) \frac{\sin^2 2\theta_{12}}{\cos 2\theta_{12}} \int_0^L dx\ V(x) \sin \phi_{x\to L}^m$$

$$\frac{d\sigma_{\nu_e e}}{dT'} / \frac{d\sigma_{\nu_\alpha e}}{dT'} \simeq 6$$

$$A_e \simeq 1.7\%$$

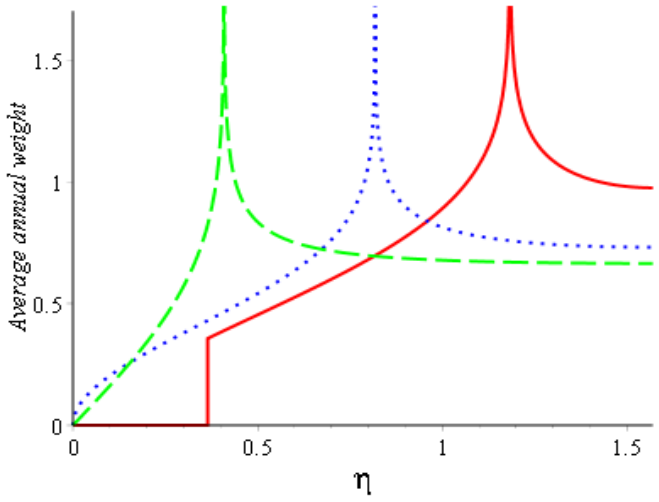


Figure: Dependance of average annual weight function on the nadir angle of neutrino trajectory($\eta$ is in radians). Outer core ($\eta < 0.58$ ) is "visible" at Homestake (SD) site about 9% of night time

$$P_{1e}/c_{13}^2 = \cos^2\theta_{12} - \frac{1}{2}\sin^2 2\theta_{12} c_{13}^2 \int_0^L dx\ V_e(x)\sin\phi^m_{x\to L},$$

where

$$\phi^m_{x\to L}(E) \equiv \int_x^L dx\ \Delta_m(x),$$

$$\Delta_m(x) \equiv \frac{\Delta m_{21}^2}{2E}\sqrt{[\cos 2\theta_{12} - c_{13}^2\epsilon(x)]^2 + \sin^2 2\theta_{12}}$$

$$\epsilon(x) \equiv \frac{2V_e(x)E}{\Delta m_{21}^2}$$

$$\approx 0.03\left(\frac{\rho(x)}{3\frac{\mathrm{g}}{\mathrm{cm}^3}}\right)\left(\frac{7.5\cdot 10^{-5}\mathrm{eV}^2}{\Delta m_{21}^2}\right)\left(\frac{E}{10\ \mathrm{MeV}}\right)\left(\frac{Y_e(x)}{0.5}\right)$$

The oscillation length can be written as

$$l_m = \frac{2\pi}{\Delta_m(x)} = l_\nu[1 + \cos 2\theta_{12} c_{13}^2\epsilon + O(\epsilon^2)].$$

$$l_\nu \approx 330\left(\frac{7.5\times 10^{-5}\mathrm{eV}^2}{\Delta m_{21}^2}\right)\left(\frac{E}{10\ \mathrm{MeV}}\right)\mathrm{km}$$